ISSN 1674-1056
http://cpb.iphy.ac.cn
http://iopscience.iop.org/cpb
中国物理 B
Chinese Physics
中国物理 Chinese Physics B

2-μm-6-μm mid-infrared supercontinuum generation in cascaded ZBLAN and As_2Se_3 step-index fibers

Jinmei Yao(姚金妹), Bin Zhang(张斌), Ke Yin(殷科), Jing Hou(侯静)

Citation: Chin. Phys. B . 2019, 28(8): 084209. **doi:** 10.1088/1674-1056/28/8/084209
Journal homepage: http://cpb.iphy.ac.cn; http://iopscience.iop.org/cpb

What follows is a list of articles you may be interested in

Monolithic all-fiber mid-infrared supercontinuum source based on a step-index two-mode As_2S_3 fiber

Jinmei Yao(姚金妹), Bin Zhang(张斌), Jing Hou(侯静)
Chin. Phys. B . 2019, 28(6): 064205. **doi:** 10.1088/1674-1056/28/6/064205

Supercontinuum generation of highly nonlinear fibers pumped by 1.57-μm laser soliton

Song-Tao Fan(樊松涛), Yan-Yan Zhang(张颜艳), Lu-Lu Yan(闫露露), Wen-Ge Guo(郭文阁), Shou-Gang Zhang(张首刚), Hai-Feng Jiang(姜海峰)
Chin. Phys. B . 2019, 28(6): 064204. **doi:** 10.1088/1674-1056/28/6/064204

Mid-infrared supercontinuum generation and its application on all-optical quantization with different input pulses

Yan Li(李妍), Xinzhu Sang(桑新柱)
Chin. Phys. B . 2019, 28(5): 054206. **doi:** 10.1088/1674-1056/28/5/054206

Supercontinuum manipulation based on the influence of chirp on soliton spectral tunneling

Saili Zhao(赵赛丽), Huan Yang(杨华), Yilin Zhao(赵奕霖), Yuzhe Xiao(肖宇哲)
Chin. Phys. B . 2018, 27(11): 114219. **doi:** 10.1088/1674-1056/27/11/114219

Intense supercontinuum generation in the near-ultraviolet range from a 400-nm femtosecond laser filament array in fused silica

Dongwei Li(李东伟), Lanzhi Zhang(张兰芝), Saba Zafar, He Song(宋鹤), Zuoqiang Hao(郝作强), Tingting Xi(奚婷婷), Xun Gao(高勋), Jingquan Lin(林景全)
Chin. Phys. B . 2017, 26(7): 074213. **doi:** 10.1088/1674-1056/26/7/074213

The 2-μm to 6-μm mid-infrared supercontinuum generation in cascaded ZBLAN and As_2Se_3 step-index fibers*

Jinmei Yao(姚金妹)[1], Bin Zhang(张斌)[1,2,3,†], Ke Yin(殷科)[4], and Jing Hou(侯静)[1,2,3,‡]

[1] College of Advanced Interdisciplinary Studies, National University of Defense Technology, Changsha 410073, China
[2] State Key Laboratory of Pulsed Power Laser Technology, Changsha 410073, China
[3] Hunan Provincial Key Laboratory of High Energy Laser Technology, Changsha 410073, China
[4] National Innovation Institute of Defense Technology, Academy of Military Sciences PLA, Beijing 100010, China

(Received 31 March 2019; revised manuscript received 8 May 2019; published online 9 July 2019)

Fiber-based mid-infrared (MIR) supercontinuum (SC) sources benefit from their spectral brightness and spatial coherence that are needed for many applications, such as spectroscopy and metrology. In this paper, an SC spanning from 2 μm to 6 μm is demonstrated in cascaded ZrF_4–BaF_2–LaF_3–AlF_3–NaF (ZBLAN) and As_2Se_3 step-index fibers. The pump source is a ZBLAN fiber-based MIR SC laser with abundant high-peak-power soliton pulses between 3000 nm and 4200 nm. By concatenating the ZBLAN fiber and the As_2Se_3 fiber, efficient cascading red-shifts are obtained in the normal dispersion region of the As_2Se_3 fiber. The spectral behavior of cascaded SC generation shows that the long-wavelength proportion of MIR SC generated in the ZBLAN fiber plays a critical role for further spectral extension in the As_2Se_3 fiber.

Keywords: supercontinuum generation, infrared lasers, fiber lasers, nonlinear

PACS: 42.55.Wd, 42.81.–i, 42.65.Ky **DOI:** 10.1088/1674-1056/28/8/084209

1. Introduction

The fiber-based supercontinuum (SC) sources offer both a broad bandwidth and a good beam quality. Particularly, SC sources in the mid-infrared (MIR) region attract enormous interest due to its potential applications in many fields, such as spectroscopic imaging,[1] trace gas detection,[2] and early-cancer diagnosis.[3] Consequently, there have been a growing number of experiments aiming at generating MIR SC using a wide variety of nonlinear fibers. Traditionally, hindered by infrared absorption of silica glass, the long-wavelength edge of SC generated in silica fibers is limited at ~ 2.7 μm.[4] Germania-core fibers have a lower phonon energy compared with silica fibers, which could further extend the long-wavelength edge of SC to about 3.6 μm.[5] For further broadening the SC spectrum, soft-glass fibers, such as fluoride fibers, tellurite fibers, and chalcogenide fibers, are much more suitable. The most common fluoride glasses are fluorozirconate glass ZrF_4–BaF_2–LaF_3–AlF_3–NaF (ZBLAN) and fluoroindate glass (InF_3). The ZBLAN glass is a mixture of ZrF_4 (53 mol.%), BaF_2 (20 mol.%), LaF_3 (4 mol.%), AlF_3 (3 mol.%), and NaF (20 mol.%).[6] To date, >10 W MIR SCs have been reported in ZBLAN glass fibers,[7–9] but the long-wavelength edge is limited at around 4.2 μm due to multiphonon absorption edge when using long fibers. The InF_3 glasses own lower phonon energy compared with ZBLAN glasses, thus the long-wavelength edge of SC generated in InF_3 fibers has been extended up to 5 μm with the output power reaching watt level.[10–12] To further boost output power and increase long term stability of fluorite fiber-based SC sources, protective methods like an AlF_3 endcap[13] need to be applied for preventing OH diffusion. Tellurite-based (TeO_2) glasses yield a higher resistance to moisture exposure than fluorides glass and it has a similar transmission band with fluorozirconate glass.[6] A watt-level MIR SC source covering 1 μm to 4.5 μm is obtained in a dispersion-zero shifted tellurite fiber with an output power of 1.2 W.[14] Recently, to improve the stability of fluoride glass fiber, a kind of fluorotellurite glass (TeO_2–BaF_2–Y_2O_3) fiber with improved chemical and thermal properties has been reported.[15] Pumped by a homemade 1980-nm chirped pulse amplification, a 10.4-W SC spanning from 947 nm to 3934 nm was obtained without obvious damage observed on the end surface of the fluorotellurite fiber for more than 10 h. Chalcogenide fibers are a kind of MIR fiber, which is based on the chalcogen elements S, Se, and Te with transmission windows of 0.8 μm–7 μm, 1 μm–10 μm, and 2 μm–12 μm, respectively. These fibers naturally yield a wide transmission window in the MIR region and a stable chemical property.[16–19]

Chalcogenide fibers usually have high zero-dispersion wavelengths (ZDWs)[16] which are far away from general fiber laser. Due to the lack of mature and reliable MIR fiber lasers, free-space pump lasers like optical parametric am-

*Project supported by the National Natural Science Foundation of China (Grant Nos. 61435009, 61235008, and 61405254), the Fund from China Scholarship Council (Grant No. 201803170210), and Hunan Provincial Innovation Foundation for Postgraduate (Grant No. CX2018B008).

†Corresponding author. E-mail: nudtzhb@163.com
‡Corresponding author. E-mail: houjing25@sina.com

© 2019 Chinese Physical Society and IOP Publishing Ltd

plifiers with ultra-short MIR pulses are widely employed in the chalcogenide fiber-based SC systems[20–25] and great progresses have been achieved using this method. The broadest MIR SC generated in a nonlinear fiber is achieved in a piece of low-loss chalcogenide fiber, which covers 2.0 μm–16.0 μm at the −40-dB level.[20] Practical applications require portable and stable SC sources which can work beyond the laboratory environment. Thus, the fiber laser with robust construction is the ideal pump source for SC generation. Cascaded SC generation in the chalcogenide fiber was proposed in 2014[26] and realized in 2016.[27] In this method, MIR soliton pulses generated in the ZBLAN fiber can further broaden toward the long-wavelength region in the chalcogenide fiber. This method can meet the need of MIR pump pulse for chalcogenide fibers and it naturally has the potential to develop an all-fiber MIR SC system. Adopting this method, an all-fiber SC laser covering 2 μm to 5 μm was obtained in an As_2S_3 step index fiber with an output power of 97.1 mW.[28] And an MIR SC up to 7 μm was obtained in a micro-structured As_2Se_3 fiber with an output power of about 6.5 mW.[27]

In this paper, an SC spanning from 2 μm to 6 μm is demonstrated in cascaded ZBLAN and As_2Se_3 step-index fibers. The ZBLAN fiber is used to build an MIR SC laser with abundant high-peak-power soliton pulses between 3000 nm and 4200 nm. By coupling solitons generated in ZBLAN fiber into the following step-index As_2Se_3 fiber, MIR pulses further broaden toward long-wavelength region in the normal dispersion region of As_2Se_3 fiber. The spectral behavior of the cascaded SC generation is investigated by changing the pump power and pump repetition rate, which shows that the long-wavelength power generated in the ZBLAN fiber plays a critical role for further spectral broadening in the As_2Se_3 fiber.

2. Experimental setup

The experimental setup for SC generation is shown in Fig. 1(a). The 1550-nm seed with 1-ns pulse duration and 10-kHz repetition rate is amplified in an erbium/ytterbium-codoped fiber amplifier (EYDFA) first and then injected into a 15-m-long single-mode fiber (SMF). An effective spectral broadening covering 1.5 μm to 2.3 μm is obtained during propagating in the SMF. Then spectral components from 1.5 μm to 1.9 μm are absorbed in a large-mode-area thulium-doped fiber (LMA-TDF) with a core/cladding diameter of 25 μm/250 μm and numerical aperture (NA) of 0.11/0.46, while the spectral components above 1.9 μm are amplified. Two mode field adapters (MFAs) are adopted in the thulium-doped fiber amplifier (TDFA) stage. The pigtail of the MFA2 has a core/cladding diameter of 7 μm/125 μm and a core NA of 0.2. The amplified pulses generated in LMA-TDF are sequentially shifted towards long wavelength region in the MFA and eventually lead to a 1.9 μm–2.7 μm SC laser.

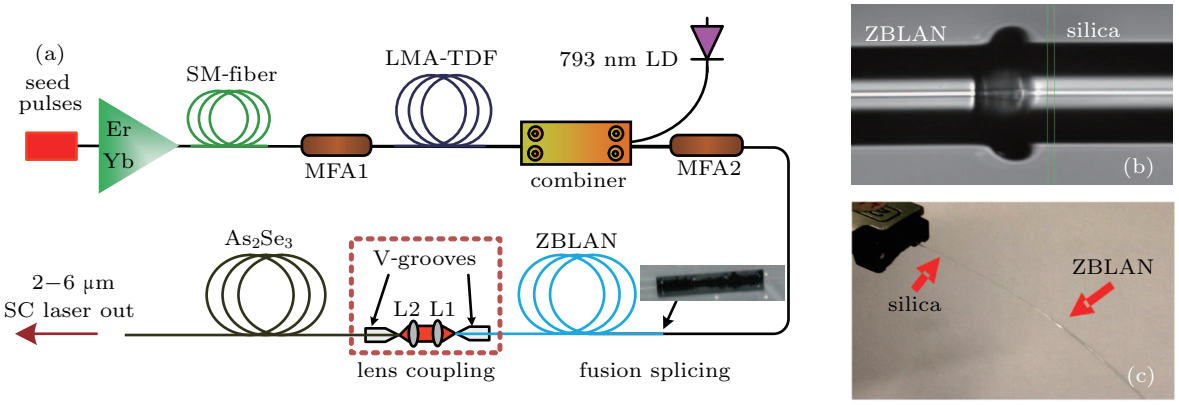


Fig. 1. (a) Experimental set-up for SC generation in cascaded ZBLAN and As_2Se_3 step-index fibers. LMA-TDF: Large mode area thulium-doped fiber; SM: Single-mode; MFA: mode field adapter. (b) Microscope and (c) photograph of fusion splicing between silica fiber and ZBLAN fiber.

To effectively broaden the MIR spectrum, a 12-m-long ZBLAN fiber with a core/cladding diameter of 9/125 μm and an NA of 0.27 is used. Low-loss fusion splice is achieved between the ZBLAN fiber and the pigtail of MFA2 by asymmetric heating method.[29] Figures 1(b) and 1(c) depict the microscope and photograph of fusion splicing between silica fiber and ZBLAN fiber, respectively. This shows that the silica fiber is wrapped by the melted ZBLAN fiber, which forms a robust fusion splicing between silica fiber and ZBLAN fiber. For protecting the fusion-spliced joint, it was mounted into an aluminum V-groove and fixed with ultraviolet curing adhesive, as shown in the inset of Fig. 1(a). The fusion splicing loss is estimated to be less than 0.1 dB after considering the linear propagation loss at around 2 μm (0.06 dB/m) and the mode mismatch loss between the pigtail of MFA2 and the ZBLAN fiber of about 0.024 dB. Based on the commercial finite element method software COMSOL Multiphysics and Sellmeier equation with the same coefficients as in Ref. [30], the calculated group velocity dispersion of the ZBLAN fiber is depicted in Fig. 2(a), which shows that it exhibits anomalous dispersion from around 1.5 μm to its multiphonon absorption edge near 4.3 μm.

To effectively confine MIR wavelengths in the core of As_2Se_3 fiber and achieve a sufficient nonlinear interaction length, a 5-m-long As_2Se_3 fiber with large core diameter of 12 μm and NA of 0.46 is used. Based on the Sellmeier equation with the same coefficients as in Ref. [31], the ZDW of the As_2Se_3 fiber is calculated at above 8 μm, as shown in Fig. 2(a). Selenium glass fibers own high refractive indices in the MIR region ($n = 2.77$ at 4 μm), thus there is about 22% optical feedback resulting from Fresnel reflection at the end facet of As_2Se_3 fiber. Angle-cleaved As_2Se_3 fiber end can prevent backward propagated light to some extent. Figure 2(b) depicts the relationship between the cutting angle of the As_2Se_3 fiber and the proportion of optical feedback that meets the total reflection condition in the core of the As_2Se_3 fiber. Due to the large NA of the As_2Se_3 fiber, a large cutting angle is required at the end facet of As_2Se_3 fiber. A cutting angle of about 12° is obtained in the experiment, which means that about 0.4% SC feedback propagates backwards in the core of As_2Se_3 fiber. The As_2Se_3 fiber is placed on an aluminum plate without applying any active cooling method. Both end facets of As_2Se_3 fiber are placed in a pair of parallel V-grooves and indium-gallium alloy is applied to strip possible cladding light.

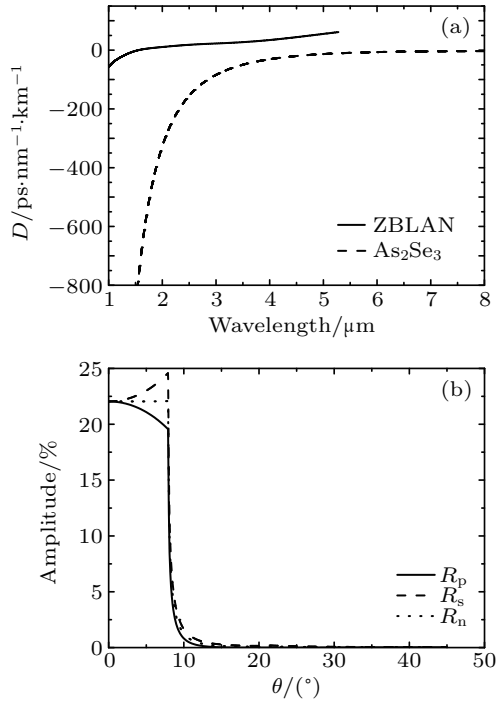


Fig. 2. (a) Calculated group velocity dispersions of the ZBLAN fiber and As_2Se_3 fiber. (b) The relationship between the cutting angle of the As_2Se_3 fiber and Fresnel reflection proportion that meets the total reflection condition in the core of the As_2Se_3 fiber. R_p, R_s, and R_n represents reflection of P-light, S-light, and total light, respectively.

To flexibly control the light spot incident into the As_2Se_3 fiber, a pair of $Ge_{28}Sb_{12}Se_{60}$ aspheric lenses with antireflection coating covering 3 μm–5 μm is adopted to achieve light coupling between the ZBLAN fiber and the As_2Se_3 fiber. The focal lengths of the lenses are 6 mm and 4 mm, respectively. A monochromator with liquid-nitrogen-cooled InSb detector and a thermal power meter are used for the measurement of spectrum and power, respectively. With the aid of a pyro-electric array camera, fundamental mode operation is ensured during the coupling alignment.

3. Results and discussion

The measured spectral evolution in the ZBLAN fiber pumped at 10-kHz repetition rate is depicted in Fig. 3(a) and the legend represents the corresponding output power. As TDFA pump power increases, the spectra of short subpulses generated in the LMA-TDF further broaden in the anomalous dispersion region of ZBLAN fiber and gradually reach ∼ 4.3 μm. Abundant high-peak-power soliton pulses located between 3000 nm and 4200 nm are the dominant components of SC generated in ZBLAN fiber. Then, the output MIR SC generated in the ZBLAN fiber is coupled into the following As_2Se_3 fiber with the pair of aspheric lenses. Due to the antireflection coating covering 3 μm–5 μm, the coupling efficiency is only ∼ 50% before the pump spectrum reaches beyond 3 μm. With the pump spectrum generated in the ZBLAN fiber reaching 4.2 μm, the coupling efficiency gradually increases to about 80%.

The spectral evolution in the following As_2Se_3 fiber is depicted in Fig. 3(b) and the legend represents output power corresponding to the pump power in Fig. 3(a). For a clear visibility, each spectrum is shifted upward by 4 dB. This shows that at the beginning, the output solitons generated in the ZBLAN fiber are too weak to induce continue SC extension in As_2Se_3 fiber. Until the output power of ZBLAN fiber is about 2.49 mW, a significant spectral broadening is observed in the As_2Se_3 fiber. As the pump power is further increased, a cascaded spectral broadening of ∼ 1000 nm is achieved in the As_2Se_3 fiber and finally an MIR SC spanning from 2 μm–6 μm is obtained with corresponding −10-dBm points from 2.2 μm to 5.5 μm. Self-phase modulation and Raman-induced frequency red-shift in the normal dispersion regime of the As_2Se_3 fiber are regarded as the dominant mechanisms responsible for cascaded spectral broadening. Obvious Stokes peaks are hard to be distinguished in the output spectra of As_2Se_3 fiber due to pump soliton pulses with different center wavelengths. Two spectral dips beyond 4 μm can be observed in the output spectrum of As_2Se_3 fiber. The spectral dip at 4.2 μm is caused by the CO_2 absorption during free space propagation of spectral measurement. The Se–H bond in the fiber causes the dip at around 4.6 μm. Near-field beam profiles detected at the output end of ZBLAN fiber and As_2Se_3 fiber are shown in the inset of Fig. 3. Although the single-mode cutoff wavelength of As_2Se_3 fiber is calculated as 7.4 μm, the fundamental mode can be excited by proper alignment.

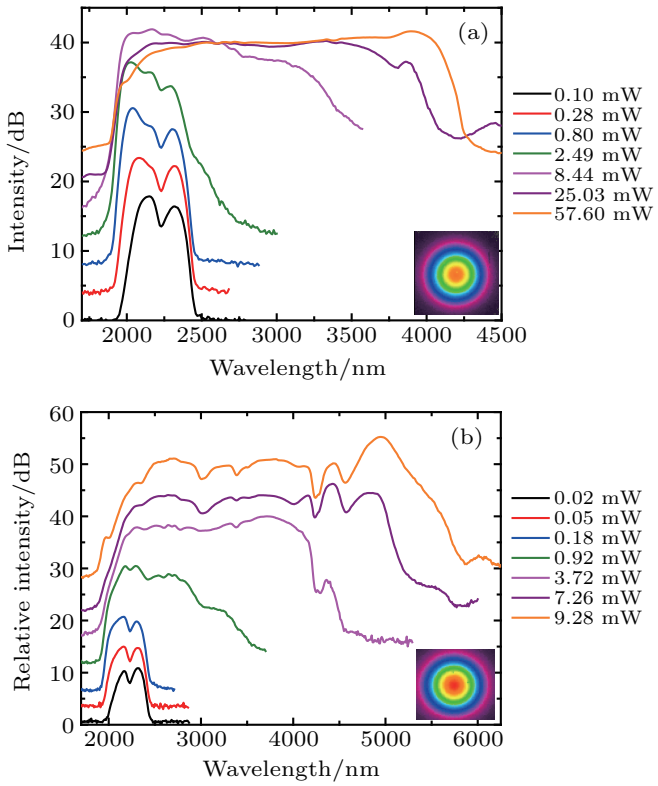


Fig. 3. Measured spectral evolution of SC generated in the (a) 12-m-long ZBLAN fiber and (b) 5-m-long As_2Se_3 fiber pumped at 10-kHz repetition rate. The legend represents output power and the insets show the corresponded SC beam profiles.

The spectral behaviors of MIR SC are investigated by changing the pump repetition rate. Figures 4(a) and 4(b) depict the comparison of SC spectra generated in ZBLAN fiber and As_2Se_3 fiber pumped at 10 kHz, 25 kHz, and 50 kHz, respectively. It shows that although 2 μm–4.2 μm SCs are obtained in the ZBLAN fiber at all pump repetition rates, the broadest cascading SC is generated in the As_2Se_3 fiber when pumped at 10 kHz. A possible explanation for this comes from the fact that solitons cannot propagate undistorted in the normal dispersion region of the As_2Se_3 fiber for a long distance. When solitons are incident into the As_2Se_3 fiber, self-phase modulation along with Raman-induced frequency red-shift leads to spectral broadening of SC. Meanwhile, time domain broadening of solitons occurs due to group dispersion. Along with the decrease of temporal intensity of pump pulse, self-phase modulation and Raman-induced frequency red-shift gradually stop in the As_2Se_3 fiber. Consequently, long-wavelength solitons with low group velocity dispersions indices in the As_2Se_3 fiber are beneficial for continuing SC broadening. Since most intense MIR solitons are obtained in the ZBLAN fiber at a repetition rate of 10 kHz, the broadest SC is generated in the As_2Se_3 fiber at 10 kHz. For effective obtaining MIR SC extension in As_2Se_3 fiber, the energy of long wavelength solitons generated in ZBLAN fiber needs to be boosted. For example, InF3 fibers with lower phonon energy in MIR region can be used to replace the ZBLAN fiber in the cascading configuration.[32] Or a piece of As_2S_3 fiber can be added as

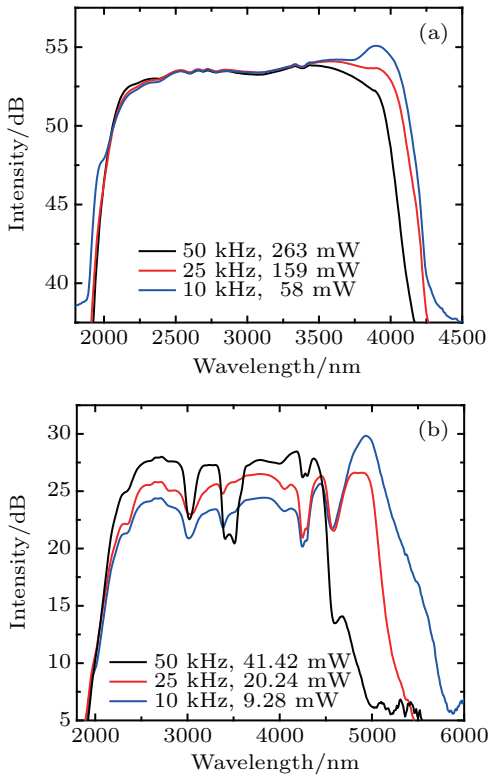


Fig. 4. Comparison of the SC spectra generated in (a) ZBLAN fiber and (b) As_2Se_3 fiber pumped at 10 kHz, 25 kHz, and 50 kHz, respectively. The legend represents the output power of the ZBLAN fiber and As_2Se_3 fiber, respectively.

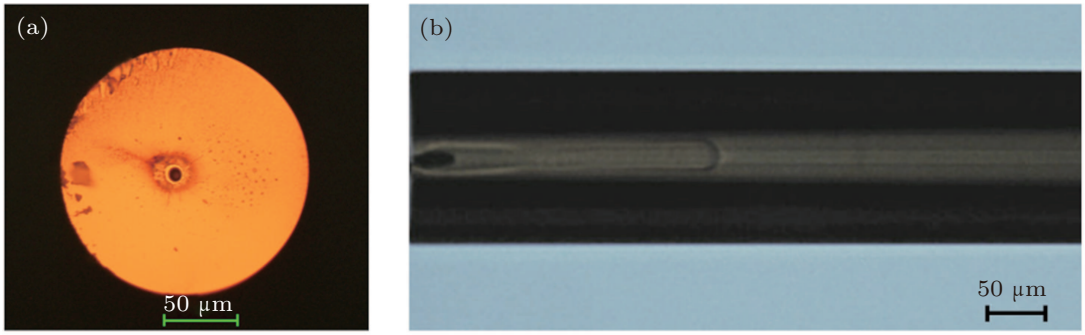


Fig. 5. (a) Damaged vertical incident facet of As_2Se_3 fiber pumped at 50-kHz repetition rate with maximum pump power of 263 mW; (b) optical microscope image of the longitudinal input segment of damaged As_2Se_3 fiber.

an intermediate fiber between the ZBLAN fiber and the As_2Se_3 fiber for further bridging the matching-gap between the pump wavelength and ZDW of the As_2Se_3 fiber, which contributes to a 1.6 μm–11 μm SC laser source in a recent report.[33]

Further SC extension is prohibited in As_2Se_3 fiber at a repetition rate of 50-kHz through raising the pump power. When the pump power is increased above 263 mW, the output power of As_2Se_3 fiber suddenly decreases unexpectedly. The optical microscope image of the incident facet of As_2Se_3 fiber shows that there is a distinct cavity like a 'crater' with a similar dimension as the core diameter of As_2Se_3 fiber, as shown in Fig. 5(a). Figure 5(b) depicts the optical microscope image of longitudinal input segment of the As_2Se_3 fiber. A $\sim$ 200-μm-long deformation and an intra-core hollow are detected in the As_2Se_3 fiber, which indicates that an eruption of the core of As_2Se_3 fiber has occurred. According to Ref. [34], a core material blast from the input facet is one of the distinct features of fiber fuse, in contrast with other fiber damage mechanisms. It is inferred that fiber fuse has occurred in the As_2Se_3 fiber.

4. Conclusion

In this paper, an MIR SC spanning from 2 μm to 6 μm is achieved in cascaded ZBLAN and As_2Se_3 step-index fibers with an output power of 9.28 mW. The spectral behaviors of the SC source are investigated by changing the pump repetition rate and the pump power, which shows that the long-wavelength power generated in ZBLAN fiber plays a critical role for further spectral broadening in As_2Se_3 fiber. A damaged cross section is observed on the incident end facet of As_2Se_3 fiber while increasing the laser repetition rate, which suggests that in order to acquire a high-power MIR SC, improved fabrication of chalcogenide fiber along with a better understanding of the damage mechanism is needed.

References

[1] Petersen C R, Prtljaga N, Farries M, Ward J, Napier B, Lloyd G R, Nallala J, Stone N and Bang O 2018 *Proc. SPIE* 10489 *Optical Biopsy XVI: Toward Real-Time Spectroscopic Imaging and Diagnosis*, February 19, 2018, San Francisco, USA, p. 1048905

[2] Cossel K C, Waxman E M, Finneran I A, Blake G A, Ye J and Newbury N R 2017 *J. Opt. Soc. Am. B* **34** 104

[3] Seddon A B 2011 *Int. J. Appl. Glass Sci.* **2** 177

[4] Swiderski J and Michalska M 2013 *Laser Phys. Lett.* **10** 035105

[5] Yin K, Zhang B, Yao J, Yang L, Liu G and Hou J 2016 *Opt. Lett.* **41** 5067

[6] Swiderski J 2014 *Prog. Quantum Electron.* **38** 189

[7] Yin K, Zhang B, Yang L and Hou J 2017 *Opt. Lett.* **42** 2334

[8] Zheng Z 2016 *Photon. Res.* **4** 135

[9] Yang W, Zhang B, Xue G, Yin K and Hou J 2014 *Opt. Lett.* **39** 1849

[10] Yang L, Zhang B, Jin D, Wu T, He X, Zhao Y and Hou J 2018 *Opt. Lett.* **43** 5206

[11] Théberge F, Bérubé N, Poulain S, Cozic S, Robichaud L R, Bernier M and Vallée R 2018 *Photon. Res.* **6** 609

[12] Liang S, Xu L, Fu Q, Jung Y, Shepherd D P, Richardson D J and Alam S U 2018 *Opt. Express* **26** 6490

[13] Aydin Y O, Fortin V, Vallée R and Bernier M 2018 *Opt. Lett.* **43** 4542

[14] Thapa R, Rhonehouse D, Nguyen D, Wiersma K, Smith C, Zong J and Chavez-Pirson A 2013 *Technologies For Optical Countermeasures X; High-Power Lasers* 2013*: Technology and Systems*, October 15, 2013, Dresden, Germany, p. 889808

[15] Yao C, Jia Z, Li Z, Jia S, Zhao Z, Zhang L, Feng Y, Qin G, Ohishi Y and Qin W 2018 *Optica* **5** 1264

[16] Shiryaev V S and Churbanov M F 2013 *J. Non-Cryst. Solids* **377** 225

[17] Asobe M 1997 *Opt. Fiber Technol.* **3** 142

[18] Ebendorff-Heidepriem H 2014 *OptoElectronics and Communication Conference and Australian Conference on Optical Fibre Technology*, July 06, 2014, Melbourne, Australia, pp. 627–629

[19] Zhang X Y, Chen F F, Zhang X H and Ji W 2018 *Chin. Phys. B* **27** 084208

[20] Zhao Z, Wu B, Wang X, Pan Z, Liu Z, Zhang P, Shen X, Nie Q, Dai S and Wang R 2017 *Laser Photon. Rev.* **11** 1700005

[21] Zhao Z, Wang X, Dai S, Pan Z, Liu S, Sun L, Zhang P, Liu Z, Nie Q and Shen X 2016 *Opt. Lett.* **41** 5222

[22] Zhang B, Yu Y, Zhai C, Qi S, Wang Y, Yang A, Gai X, Wang R, Yang Z and Luther-Davies B 2016 *J. Am. Ceram. Soc.* **99** 2565

[23] Cheng T, Nagasaka K, Tuan T H, Xue X, Matsumoto M, Tezuka H, Suzuki T and Ohishi Y 2016 *Opt. Lett.* **41** 2117

[24] Petersen C R, Møller U, Kubat I, Zhou B, Dupont S, Ramsay J, Benson T, Sujecki S, Abdel-Moneim N and Tang Z 2014 *Nat. Photon.* **8** 830

[25] Wang Y, Dai S, Xin H, Zhang P, Liu Y, Wang X and Sun S 2018 *Opt. Commun.* **410** 410

[26] Irnis K, Christian Rosenberg P, Uffe Visbech M L, Angela S, Trevor B, Laurent B, David M, Moselund P M and Ole B 2014 *Opt. Express* **22** 3959

[27] Petersen C R, Moselund P M, Petersen C, Møller U and Bang O 2016 *Opt. Express* **24** 749

[28] Yin K, Zhang B, Yao J, Cai Z, Liu G and Hou J 2017 *J. Lightwave Technol.* **35** 4535

[29] Yin K, Zhang B, Yao J, Yang L, Chen S and Hou J 2016 *Opt. Lett.* **41** 946

[30] Brown R N and Hutta J J 1985 *Appl. Opt.* **24** 4500

[31] Dantanarayana H G, Abdelmoneim N, Tang Z, Sojka L, Sujecki S, Furniss D, Seddon A B, Kubat I, Bang O and Benson T M 2014 *Opt. Mater. Express* **4** 1444

[32] Théberge F, Bérubé N, Poulain S, Cozic S, Châtigny S, Robichaud L R, Pleau L P, Bernier M and Vallée R 2018 *Opt. Express* **26** 13952

[33] Martinez R A, Plant G, Guo K, Janiszewski B, Freeman M J, Maynard R L, Islam M N, Terry F L, Alvarez O, Chenard F, Bedford R, Gibson R and Ifarraguerri A I 2018 *Opt. Lett.* **43** 296

[34] Xing S, Kharitonov S, Hu J and Brès C S 2018 *Opt. Lett.* **43** 1443